Author

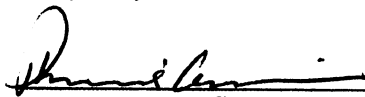Aaron R. Wood, Mary J. Kraus, and Philip D. Gingerich

Title

Mammal-bearing fluvial conglomerates in the Paleocene-Eocene boundary interval
(Willwood Formation, Bighorn Basin, Wyoming)
and quantification of down-slope contamination

Submitted for Publication in:

Palaeogeography, Palaeoclimatology, Palaeoecology

**in lieu of thesis in partial fulfillment
of the requirements for the degree of
Master of Science in Geology
Department of Geological Sciences
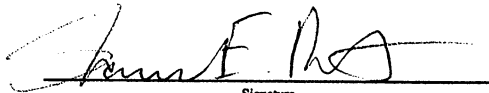The University of Michigan**

Accepted by:

Signature	Name	Date
(signature)	PHILIP D. GINGERICH	12/4/06
(signature)	Shanan E. Peters	12/7/06
R.C. E. *(Department Chair)*	R.C. Ewing	12/8/06

I hereby grant the University of Michigan, its heirs and assigns, the non-exclusive right to reproduce and distribute single copies of my thesis, in whole or in part, in any format. I represent and warrant to the University of Michigan that the thesis is an original work, does not infringe or violate any rights of others, and that I make these grants as the sole owner of the rights to my thesis. I understand that I will not receive royalties for any reproduction of this thesis.

☑ Permission granted.

☐ Permission granted to copy after: _____ Date

☐ Permission declined.

(Author Signature)

Aaron Wood

Mammal-bearing fluvial conglomerates in the Paleocene-Eocene boundary interval

(Willwood Formation, Bighorn Basin, Wyoming)

and quantification of down-slope fossil contamination

Aaron R. Wood, Mary J. Kraus, and Philip D. Gingerich

Abstract.--- The early Wastachian mammalian fauna coincident with the Paleocene-Eocene thermal maximum (PETM) includes several lineages that exhibit significantly smaller body sizes compared to immediately preceding and succeeding relatives, interpreted as either ecological replacement of larger species by smaller congeners or as evolutionary dwarfing in response to raised temperatures during the PETM. These competing hypotheses have been complicated by rare contemporary occurrences of closely-related taxa similar in body size to descendants from overlying strata. Such rare occurrences of taxa commonly found in overlying beds may be the result of down-slope fossil contamination, the likelihood of which can be evaluated by documenting potential contaminant source horizons in conjunction with modeling the effects of down-slope contamination. Here we describe the occurrence of vertebrate concentrations within conglomerates that erosionally rest upon strata encompassing the Paleocene-Eocene Thermal Maximum (PETM) and interpret them as the results of trunk channel migration and sheetflooding into an abandoned portion of an avulsion belt. The contribution of contamination to faunal assemblages was modeled using parameters aspects of the conglomerates and associated fossils, indicating the rare occurrences of larger, closely-related taxa may be explained by contamination alone. Overall, the results of this study indicate that the alluvial architecture of overlying strata can inform biostratigraphers about the potential for fossil contamination, and that the complications imposed by fossil contamination can be quantitatively assessed.

Introduction

Gravity orders strata and their contained organic remains vertically as they are deposited through time, but also causes fossils that later erode from host strata to fall down-slope onto older beds. Here we document the occurrence of down-slope fossil contamination from highly fossiliferous conglomeratic beds and use the derived information to model such contamination in a setting of wide interest within the Paleocene-Eocene thermal maximum (PETM). During this event, several lineages appear to have responded to elevated temperatures through either emigration and replacement by smaller, related species or by evolving smaller body sizes (dwarfing). The latter hypothesis is complicated by recovery of rare, closely-related, and seemingly contemporary taxa that are common in overlying strata. Our model enables us to evaluate the likelihood that the rare and complicating records result from down-slope contamination whereas our interpretations of the processes involved in conglomerate deposition will assist biostratigraphers in assessing the potential for contamination elsewhere.

The PETM was a global warming event (~ 3-7 °C increase in temperature) that occurred nearly 55.5 Mya and is associated with a massive influx of isotopically light carbon into the atmosphere evident through a carbon isotope excursion (Gingerich 2003; Koch et al. 2003). This interval also includes the first appearance of artiodactyls, perissodactyls, and primates worldwide, although this is best documented in the earliest Eocene Wasatchian-0 (Wa-0) strata of the Bighorn and Clarks Fork Basins, northwestern Wyoming. Several mammalian lineages exhibit small body sizes during the PETM, and whether these size reductions are the result of ecological replacement or evolutionary

dwarfing remains unclear. In his discussion of body size trends in the Ectocion and Hyracotherium lineages during the Wa-0 interval, Gingerich (2003) noted that a few specimens of the larger species of each lineage, Ectocion osbornianus and Hyracotherium grangeri, were found with more abundant and smaller taxa, Ectocion parvus and Hyracotherium sandrae. The co-occurrence of the smaller and larger species of Ectocion during the PETM supports ecological replacement to the extent that the larger species were rare, but Gingerich (2003) pointed out the possibility that the small sample sizes of E. osbornianus represent contaminants from younger intervals.

However, small sample sizes of problematic taxa alone are insufficient to invoke contamination as a significant contributor to fossil assemblages. The alluvial architecture of overlying strata must be considered when assessing the potential for contamination, and evidence for contamination should include documented contaminant source horizons and known spatial distribution of displaced fossil contaminants. Once a source horizon is known, the characteristics of its lithology may allow biostratigraphers to predict the occurrence of contamination in other localities.

Here we document the occurrence of two highly fossiliferous Wa-1 conglomerates that directly overlie two of the most productive Wa-0 localities in the northwestern Bighorn Basin. These conglomerates contain concentrations of characteristically black Wa-1 fossils which weather out and can be traced many meters downslope, surficially mixed with Wa-0 faunal remains. Lithologies and depositional environments are described along with the associated vertebrate fossils. These horizons allow for refinement of the Wa-0/Wa-1 boundary in the Wa-0 type section of the northwestern Bighorn Basin and provide an impetus for estimating the contribution of

contamination to species' proportions within other assemblages. Such estimates can then be applied to the dwarfing/replacement hypotheses associated with the Wa-0 fauna. This is not a full evaluation of the competing hypotheses, but a quantitative evaluation of the important complication of down-slope contamination that will be applicable in other settings as well.

Wa-0 Localities of Polecat Bench

The Wa-0 fauna of the Bighorn and Clarks Fork Basins is preserved within the Willwood Formation, an alluvial formation deposited by meandering systems during the latest Paleocene and earliest Eocene, and the Wa-0 fossil-bearing localities of interest to this study form a northwest-southeast trend along the southern tip of Polecat Bench, a Pleistocene river terrace (Fig. 1). These localities are part of the Sand Coulee (SC) series of the University of Michigan Museum of Paleontology (UMMP) fossil vertebrate localities and include the localities SC-69, SC-121, SC-308, and SC-67. Gingerich (1989) provided a general description of these localities in addition to the description of the faunas contained therein.

A multistory sheet sandstone complex runs throughout SC-69, SC-121, and SC-308 and pinches out in the western margin of SC-67 (Fig. 2). This sheet sandstone was deposited by a trunk channel, and the multi-story character of the complex indicates the trunk channel was confined to a single meanderbelt for a significant length of time before avulsion events allowed the channel to establish in other areas of the floodplain (Kraus 1980, 2001). This sheet sandstone has an exposed lateral extent of 650 m and a maximum thickness of 10 m. Paleocurrent data from 50 measurements of large-scale

crossbedding indicate that paleoflow of the sheet sandstone was to the north-northeast (mean azimuth of 11.47°). Gingerich (2001) termed this sheet sandstone the "Upper Boundary Sandstone" when including it in his SC-121 section and described it as being part of the Clarks Fork sheet sandstone described by Kraus (1979, 1980) separated from the "Lower Boundary Sandstone" by Wa-0 strata within the Clarks Fork sheet sandstone.

In the SC-121 stratigraphic section of Gingerich (2001), the age of the "Upper Boundary Sandstone" (UBS) remained uncertain due to a lack of diagnostic fossils of either Wa-0 or Wa-1 age. However, the UBS lies erosionally on a thick red paleosol named Upper Double Red B, which is Wa-0 in age as indicated by the vertebrate fossils it produces. The known position of the earliest Wa-1 strata as reported by Gingerich (2001) is nearly 10 m above the UBS and just below another thick red paleosol named Top Red A.

During the summers of 2004-05, UMMP field crews collected 67 vertebrate fossils with distinctive dark gray bone and black enamel from localities SC-69 and SC-308. Nearly half of these fossils were found laying on exposures of paleosols known to be Wa-0 in age; however, this type of fossil preservation is not known from Wa-0 strata. The source of the 21 black fossils found in SC-308 was discovered to be a cross-stratified, carbonate nodule conglomerate with a coarse sand matrix within the UBS. This type of conglomerate is a minor component throughout the UBS and is interpreted to be a channel lag deposit of a trunk river (Kraus 1979). Whereas a small number of black dental specimens in SC-69 were discovered weathering out of channel lag deposits within the overlying UBS, the majority of the black specimens were found weathering out of a carbonate nodule conglomerate below the UBS. That lower conglomerate has features

unlike the channel lag conglomerates in the UBS, suggesting that different depositional processes were involved.

Lithologies and Interpretations

Two types of conglomerate are recognized from the Polecat Bench. The recognition of these conglomerates and their hypothesized origins are based upon characteristics of the conglomerates themselves, such as clast/matrix composition and sedimentary structures, as well as characteristics of the adjacent lithologies (Table 1).

UBS Channel Lag Conglomerates – Description & Interpretation

The UBS channel lag conglomerates are clast-supported with a matrix of medium-coarse sand with little to no clay and silt. Larger grains commonly consist of abraded soil carbonate nodules and mudclasts; however, granule-pebble sized chert grains can be locally abundant. These conglomerates exhibit a crude cross-stratification (Fig. 3A), commonly with the highest concentration of coarse grains near the base of individual foresets. Channel lag conglomerates commonly grade into large-scale trough cross-stratified sandstone and are found above scours into low angle cross-stratified sandstone (Kraus 1979).

Kraus (1979, 1980) interpreted channel lag conglomerates as representing erosion and deposition at the deepest part of the meandering river channel. Abraded soil nodules indicate reworking of older, pedogenically modified overbank deposits, and the cross-bedded appearance may be due to overlapping scour fills as the channel progressed laterally through the flood plain. The gradational contact between the channel lag conglomerates and large scale trough cross-stratified sandstones indicates that the

conglomerates are part of the fining upwards sequence associated with meandering river systems (Walker and Cant 1984) where the cross-stratified sandstones represent the lateral accretion of point bars. Kraus (1979) interpreted the low angle cross-stratified sandstones to represent upper flow regime deposition of sediment at the tops of point bars during floods. The common presence of channel lag conglomerates above scours into these low angle cross-stratified sandstones implies that rivers often eroded and reworked the upper portions of older stories in the sandstone complex, which further suggests that conglomerate deposition occurred within or near the confines of the river channel.

<u>SC-69 Carbonate Nodule Conglomerate – Description</u>

The SC-69 conglomerate is not part of a sheet sandstone complex. It is underlain by heterolithic deposits and overlain by low-angle cross-stratified sandstone of the UBS. It is more fossiliferous than the UBS conglomerate and lies ~ 1 m above Wa-0 paleosol deposits. Attributes of the SC-69 conglomerate indicate a different depositional history compared to the UBS conglomerates.

The SC-69 conglomerate is clast-supported with pedogenic carbonate nodules representing greater than 90% of the framework clasts. Other framework clasts include mudclasts, vertebrate fossils, and calcified rhizolith fragments. The matrix is higher in clay content compared to the UBS channel lag conglomerates. Poorly defined beds that are 10-15 cm thick are present with larger carbonate nodules concentrated at their base (Fig. 3B). Some exhibit normal grading of carbonate nodules, and couplets with a basal coarse grained (pebble-cobble size) bed overlain by a finer (granule-pebble size) beds are present locally (Fig. 3C). Thin claystone lenses (~ 4 cm thick) occur within the

conglomerate and they often exhibit soft sediment deformation and/or differential compaction.

Fossils exhibit preservation styles indicative of complex and varied taphonomic histories. The majority of the identifiable fossils are individual teeth or tooth fragments, but four dentary fragments and a single astragalus were also found. Several of the fossils exhibit carbonate encrustation, suggesting that some remains were incorporated into soil horizons before subsequent reworking. Most teeth lack roots and exhibit abraded fractures indicative of fluvial transport (Badgley 1986). In addition, some fossils have been extensively abraded into discs (Fig. 4A) and spheroids (Fig 4B), shapes that are indicative of significant periods of transport. The most complete specimen (Fig. 4D) is a partial dentary that has been cracked, distorted, and cemented together with a sandy matrix similar to that of the conglomerate. Several small (< 2 mm in length), delicate teeth and dentary fragments were preserved in the conglomerate with little to no abrasion or encrustation and probably did not experience long transport.

The conglomerate progressively thickens to the northwest from 10 cm in the center of SC-69 to > 1 m at the northwest margin. Bedding, orientation, and number of beds change along this southeast-northwest transit as well. In the center of SC-69, only 1-2 beds of conglomerate are present and have a nearly horizontal orientation. The number and inclination of the conglomerate beds increase northwestward reaching a maximum composite thickness of > 1 m and a maximum dip of 23° at the northwestern-most exposure, creating a cross-bedded appearance (Fig. 3B). The inclination of the beds at this exposure shallows near the contact with underlying lithologies.

The conglomerate exposure shown in Fig. 5 is oblique to paleoflow as measured from UBS cross-strata, but bedding in the conglomerate suggests that the conglomerate was deposited by flow to the northwest (from right to left in the figure). The conglomerate in this exposure is ribbon shaped with a thin lateral equivalent extending to the southeast. The northwestern end of the conglomerate is covered; however, 60 m northwest of SC-69, the gray silty mudstone (G) below the conglomerate is directly overlain by the sandstone (L) immediately above the conglomerate, implying a lack of a thin lateral equivalent to the northwest. The conglomerate remains 1 m in thickness in an exposure ~ 100 m north from the cross section shown in Fig. 5, suggesting that the ribbon portion of the conglomerate extends to the north.

The most distinctive feature of the SC-69 conglomerate is that it lies above an interval of fine-grained deposits most of which show little to no pedogenic alteration and that are interbedded with sandstone lenses (i.e. a heterolithic interval) (Fig. 3D). Most of the fine-grained deposits are gray silty-mudstones with thin beds that exhibit yellow-brown masses and slickensides, indicating only weak pedogenic alteration and periodic wetting and drying of sediments (Kraus and Hasiotis 2006). Several channel fills are present in the interval (Fig. 3D and 5). The lower parts of the fills are dominated by medium-grained sandstone with ribbon geometries, and dark gray claystone forms the upper parts of the channel fills. The thickest portion of the SC-69 conglomerate lies immediately above a channel fill that is one of the thickest within the heterolithic interval. The mudstone part of this channel fill shows no obvious pedogenic alteration. Where the conglomerate is thin, the underlying channel fills are also thin and the mudstone parts of the fills show more extensive pedogenic alteration.

The heterolithic interval lies immediately above a thick red/purple paleosol couplet that correlates to the paleosol known as Upper Double Red B from the composite southern Polecat Bench section of Gingerich (2001).

SC-69 Carbonate Nodule Conglomerate and Heterolithic Interval – Interpretation

Following Kraus and Aslan (1993) and Kraus (1996), the heterolithic interval below the SC-69 conglomerate is interpreted as the deposits of an avulsion belt. The ribbon-shaped channel deposits represent the splay channels in the evolving splay complex whereas the gray silty mudstones surrounding the ribbon sands are interpreted as overbank deposits of the splay channels. The relict bedding and poor soil development indicate that the sedimentation rate was high and/or soils were poorly drained that these overbank deposits could not develop strong soil profiles as did the underlying red/purple paleosol couplet (Kraus 1996, 2001).

The channel fills that underlie the thin parts of the conglomerate record shallow channels that must have experienced periodic subaerial exposure based on the degree of pedogenic development of the mudrock part of the fill. The thick channel fill that underlies the thick part of the conglomerate contains mudstone that lacks pedogenic modification, indicating it was not subaerially exposed for long periods of time (Kraus and Davies-Vollum, 2004). Instead, the fine sediments may have settled from standing water in the splay channel. These different types of channel fill suggest that, when the conglomerate was deposited, the floodplain had irregular topography with linear depressions left by abandoned channels that had not yet filled completely.

The SC-69 conglomerate is interpreted to have been deposited by sheetflooding into that local topographic depression. The meter-thick portion of the conglomerate

extends northward implying that the abandoned splay channel extended northward from SC-69. However, the bedding of the conglomerate is oblique to the channel cross section, suggesting that the conglomerate was deposited by water flowing across, not parallel, to the long axis of the abandoned channel. The thin beds of coarse grained material in combination with the relatively wide area of exposure indicate that high velocity flood waters spread in sheets over the floodplain in a splay. Individual beds of the conglomerate may have been deposited by separated pulses of the same flood event or as portions of the levee and splay deposits were weakened and entrained at different times during a single flood. However, the occurrence of multiple conglomeratic beds and the presence of interbedded claystone lenses within the conglomerate suggest that the conglomerate in SC-69 represents several flood events.

The fossil content of the sheetflood and channel lag conglomerates appear to be a mixture of typical Wa-0 and Wa-1 faunas (Tables 2 and 3). These conflicting ages can be accommodated by the complex taphonomic histories evident from the fossil themselves, providing the possibility that the channels that produced the respective conglomerates reworked strata of both Wa-0 and Wa-1 age. Nonetheless, a Wa-1 age is the best age assignment for each conglomerate. Consequently, the Wa-0/Wa-1 boundary can be extended to the base of the purple-4 paleosol in the composite southern Polecat Bench section of Gingerich (2001).

Estimated Species Proportions due to Contamination

Wa-1 fossils derived from the described conglomerates were found intermixed with Wa-0 fossils at SC-69 and SC-308, providing a documented case of fossil

contamination of Wa-0 assemblages. The majority of Wa-0 localities in the Clarks Fork and northwestern Bighorn Basins are overlain by sheet sandstone complexes and heterolithic deposits similar to those containing the two conglomerates, prompting the question of how much of a fossil assemblage is contributed by contamination from overlying strata. A more directed question can be asked in the context of the dwarfing/replacement hypotheses discussed above: Can the presence of the rare, larger-bodied congenerics, Ectocion osbornianus and Hyracotherium grangeri, in Wa-0 assemblages be explained by contamination from overlying strata?

At a particular stratigraphic level, the number of fossils collected can be expressed as the sum of the number originating from that level and the number contributed by contamination from above. A given taxon represents a certain proportion (*p*) of an assemblage, and, therefore, the above sum can be specified for a taxon by multiplying each factor by the appropriate proportion:

$$N \cdot p_i = (N - N_c) \cdot p_{true} + N_c \cdot p_{i+1}$$ Equation 1

where N = total number of fossils collected,
 N_c = number of fossils from contamination,
 p_i = observed proportion at level$_i$,
 p_{i+1} = observed proportion at level$_{i+1}$, and
 p_{true} = true proportion at level$_i$.

Eq. 1 can be rearranged into the following:

$$p_i - \frac{N_c}{N} \cdot p_{i+1} = \frac{(N - N_c)}{N} \cdot p_{true}$$ Equation 2.

The quantity N_c/N reflects the probability of contamination from overlying stratigraphic levels (i.e. P(C)) and can be estimated using an exponential distribution, because a fossil has a finite probability of being transported over a distance down slope from its level of origin in a given increment of time. Using an exponential distribution

requires either direct rate measurements or knowledge of the average distance traveled by a fossil from its level of origin, which can be measured empirically. Once this average distance is known, the probability of a fossil reaching a certain distance down slope can be calculated using the following equation:

$$P(C) \sim \int_{y_1}^{y_2} (1/\theta) e^{-y/\theta} \, dy$$

Equation 3

where θ = the average distance from the level of origin.

This estimate of P(C) is greatly simplified since it assumes that all fossils were exposed and allowed to move over the same time interval and that there has been no attrition due to fossil destruction during transport.

Equations 2 & 3 were combined in order to investigate whether or not the presence of Ectocion osbornianus and Hyracotherium grangeri in the Wa-0 fauna might be due to contamination from overlying Wa-1 strata. The stratigraphic ranges of each species were subdivided into 20 m intervals, and faunal proportions were calculated for each interval using the UMMP collections. An interval thickness of 20 m was used in order to study the Wa-0 biozone as a single interval, which is ~ 20 m in the Clarks Fork and northwestern Big Horn Basins.

The center of each interval was taken to be the average level of origin for each fossil, and fossils were counted as contaminants if they fell to any point within the underlying interval (Fig. 6A). In other words, the integral in Eq. 3 was evaluated from 10-30 m. The average distance a fossil travels from its level of origin (θ) was estimated using the mean distance SC-69 and SC-308 conglomerate fossils were found below the

their respective conglomerates (4.3 m). With this framework, the presence of a taxon in

interval$_i$ can be explained by contamination from above if the following criterion is met:

$$p_i - P(C) \cdot p_{i+1} \leq 0 \qquad \qquad \text{Equation 4.}$$

A one-sided 95% confidence interval was calculated for $P(C) \cdot p_{i+1}$ by using a binomial

distribution to create 1000 random deviates of the observed p_{i+1}. The mean value and

95% upper bound were calculated for each interval$_{i+1}$, and the upper bound was used in

Eq. 4. For example, at a particular interval i, a taxon represents 1% of the fauna (p_i =

0.01), but in the succeeding level the taxon represents 10% of the fauna (p_{i+1} = 0.1).

After generating a confidence interval for p_{i+1} and evaluating Eq. 3 from 10-30 m, the

95% upper bound for the expected contaminant contribution in interval i is ~ 0.011,

meeting the criterion in Eq. 4.

Based on Eq. 4, the expected contaminant contribution to p in interval i is

dependent on the species proportion in interval $i+1$, or p_{i+1}, which allows some basic

predictions to be made. First, last occurrences of a species will have a zero contaminant

contribution since the species was not found in any overlying level, despite there being a

finite probability that the specimen(s) defining the last occurrence is a contaminant and

is, therefore, at a level lower than the actual last occurrence. Second, a rare species at a

given level will not necessarily be found to be a contaminant unless the species represents

a sufficiently large proportion of the fauna in the overlying interval. Similarly, the

proportion due to contamination for a particular time interval may be artificially inflated

if p_{i+1} is unusually large (Fig. 6B-C).

Figure 7 shows the results for <u>Ectocion osbornianus</u> and <u>Hyracotherium grangeri</u>.

In each graph, the difference between the observed p and confidence interval upper

bound is plotted. If this difference is $\leq$ zero, then the presence of the respective species is very likely to reflect contamination (i.e. $p_{true} = 0$). In addition, the difference between p_{i+1} and the median p is plotted on each graph in order to detect unusually high species proportions in the overlying intervals. If unusually high species proportions have artificially inflated the expected contaminant contribution, one would expect a negative correlation between the two lines. If the presence of a species is due to contamination, the expected p_{i+1} can be calculated by solving Eq. 2 for p_{i+1} and setting p_{true} to zero. The expected p_{i+1} can then be compared to the observed p from the two conglomerates overlying SC-69 and SC-308 to check the validity of the results.

All intervals in the Ectocion osbornianus range have positive values, except for the interval between 1280 and 1300 m and the Wa-0 interval. The majority of the specimens from this interval were collected from locality SC-188, a quarry site with a predominance of small-bodied mammals (Rose, 1981). Based on the entire stratigraphic range, the median species proportion for E. osbornianus is 0.118 whereas at SC-188 E. osbornianus has a species proportion of only 0.003, suggesting that there is either a bias against large-bodied mammals in this interval or a bias against small-bodied mammals in all other intervals. The observed p in the Wa-0 interval is half the contamination upper bound, meaning it is conceivable that the presence of E. osbornianus in Wa-0 could be explained by contamination alone. The correlation of 0.51 indicates that the calculations were not biased by unusually high species proportions in overlying intervals. Furthermore, the expected p_{i+1} based on the observed p for E. osbornianus in the Wa-0 interval is 0.048, which is less than the observed p for E. osbornianus in the two conglomerates ($p = 0.071$).

Similarly, all intervals of the Hyracotherium grangeri have positive values except for the Wa-0 interval. The observed Wa-0 species p is an order of magnitude smaller than the contamination upper bound. No strong biases are likely because the species proportion of the overlying interval is typical for Wa-1 and the correlation is not negative. The expected p_{i+1} is 0.074, nearly half of the observed p for H. grangeri in the two conglomerates overlying SC-69 and SC-308 ($p = 0.143$). Again, according to this test, it is possible that the presence of H. grangeri in some Wa-0 localities can be explained by contamination from overlying beds.

Discussion

The model results indicate that the presence of both Ectocion osbornianus and Hyracotherium grangeri in Wa-0 fossil assemblages is likely the result of down-slope contamination, meaning that these larger species did not coexist with the more abundant and smaller species, Ectocion parvus and Hyracotherium sandrae, during the PETM. These results are congruent with the evolutionary dwarfing hypothesis for small body sizes, which can be refuted by well documented occurrences of the larger taxa. However, the model results do not refute the ecological replacement hypothesis either, because the smaller species may have replaced or displaced the larger species until the latter were completely absent from the basin. Overall, the model results weaken those replacement hypotheses that require the coexistence of rare, large-bodied species and abundant, small-bodied species during the PETM and indicate that occurrence data is not sufficient to address this question.

Admittedly, the model used to evaluate down-slope contamination is relatively simplistic and serves only as a starting point for quantifying the contribution of contamination to fossil assemblages. Future versions of the model should include parameters based on aspects of the individual localities, including the thickness of strata in each locality, topography, and stratigraphic levels of individual fossiliferous horizons. More importantly, time dependent parameters, such as the time since exposure, erosion rates, and fossil destruction rates, should be incorporated. However, these parameters require empirical measurements, meaning that the contribution of contamination may be more realistically estimated at the locality scale and not at the scale of a species' stratigraphic range.

The model produces conservative estimates of fossil contamination, because it does not evaluate the potential for contamination from within a given interval. Depositional processes, such as channel migration and sheetflooding, can produce laterally-equivalent, temporally-disparate lithologies by simultaneously depositing new sediment while eroding older floodplain deposits or by infilling local topographic lows previously scoured by fluvial processes. Laterally-equivalent, temporally-disparate lithologies, such as the Wa-1 conglomerates and the Wa-0 paleosols (Fig. 2), contain fossils of various ages at the same stratigraphic position and complicate observations of faunal succession. Therefore, our results are likely underestimates of the effects of contamination on Wa-0 fossil assemblages, providing further support for the hypothesis that Ectocion osbornianus and Hyracotherium grangeri did not coexist with the smaller congeners during the PETM.

Conclusion

Fossil fragments make up a significant portion of the coarse-grained fraction of any deposit, and understanding the processes that concentrate and deposit coarse grains within the context of a given formation or facies can inform biostratigraphers about the potential for faunal contamination. In the context of the Willwood Formation, flash flooding in addition to channel migration can lead to significant soil erosion, reworking of older flood-plain deposits, and local concentration of fossil fragments, complicating observations of biotic succession. Fortunately, these processes leave distinct features that can be identified if the alluvial architecture is taken into account when collecting fossil specimens.

The results of this study imply that the probability of fossil contamination on Willwood strata of Wa-0 age is rather high, which complicates our observations and hypotheses concerning fossil organisms during the PETM. However, quantitative estimates of the probability of contamination permit corrections for this potential source of bias. The model used in this study indicates that the presence of <u>Ectocion osbornianus</u> and <u>Hyracotherium grangeri</u> in Wa-0 faunas could be due to contamination. Although these results do not support either ecological replacement or dwarfing for the reduced size in <u>Ectocion</u>, they do weaken any hypothesis dependent on co-occurrence of the two species during the Wa-0 interval.

Acknowledgements

would also like to thank Thomas P. Eiting and Brady Z. Foreman for their assistance in the field. Field work was conducted with support from NSF EAR-0125502.

References

Badgley, C. 1986. Taphonomy of mammalian fossil remains from Siwalik rocks of Pakistan. Paleobiology 12: 119-142.

Gingerich, P. D. 1989. New earliest Wasatchian mammalian fauna from the Eocene of Northwestern Wyoming: Composition and diversity in a rarely sampled high-floodplain assemblage. University of Michigan Papers on Paleontology 28: 97 pp.

---. 2001. Biostratigraphy of the continental Paleocene-Eocene boundary interval on Polecat Bench in the northern Bighorn Basin. *In* P. D. Gingerich, ed. Paleocene-Eocene stratigraphy and biotic change in the Bighorn and Clarks Fork Basins, Wyoming. University of Michigan Papers on Paleontology 33: 37-71.

---. 2003. Mammalian responses to climate change at the Paleocene-Eocene boundary: Polecat Bench record in the northern Bighorn Basin, Wyoming. *In* P. D. Gingerich, B. Schmitz, E. Thomas, and S. L. Wing, eds. Causes and consequences of globally warm climates in the early Paleogene. Geological Society of America Special Paper 369: 463-478. Geological Society of America, Boulder, Colo.

Koch, P. L., W. C. Clyde, R. P. Hepple, M. L. Fogel, S. L. Wing, and J. C. Zachos. 2003. Carbon and oxygen isotope records from paleosols spanning the Paleocene-Eocene boundary, Bighorn Basin, Wyoming. *In* P. D. Gingerich, B. Schmitz, E. Thomas, and S. L. Wing, eds. Causes and consequences of globally warm climates in the early Paleogene. Geological Society of America Special Paper 369: 49-64. Geological Society of America, Boulder, Colo.

Kraus, M. J. 1979. The petrology and depositional environments of a continental sheet

    sandstone: The Willwood Formation, Bighorn Basin, Wyoming. MS thesis,

    University of Wyoming, 1-106.

---. 1980. Genesis of a fluvial sheet sandstone, Willwood Formation, northwest

    Wyoming. *In* P. D. Gingerich, ed. Early Cenozoic paleontology and stratigraphy

    of the Bighorn Basin, Wyoming. University of Michigan Papers on Paleontology

    24: 87-94.

---. 1996. Avulsion deposits in lower Eocene alluvial rocks, Bighorn Basin, Wyoming.

    Journal of Sedimentary Research 66: 354-363.

---. 2001. Sedimentology and depositional setting of the Willwood Formation in the

    Bighorn and Clarks Fork Basins. *In* P. D. Gingerich, ed. Paleocene-Eocene

    stratigraphy and biotic change in the Bighorn and Clarks Fork Basins, Wyoming.

    University of Michigan Papers on Paleontology 33: 15-28.

Kraus, M. J. and A. Aslan. 1993. Eocene hydromorphic paleosols: Significance for

    interpreting ancient floodplain processes. Journal of Sedimentary Petrology 63:

    453-463.

Kraus, M. J. and K. S. Davies-Vollum. 2004. Mudrock-dominated fills formed in

    avulsion splay channels: Examples from the Willwood Formation, Wyoming.

    Sedimentology 51: 1127-1144.

Kraus, M. J. and S. T. Hasiotis. 2006. Significance of different modes of rhizolith

    preservation to interpreting paleoenvironmental and paleohydrologic settings:

    Examples from Paleogene paleosols, Bighorn Basin, Wyoming, U.S.A. Journal

    of Sedimentary Research 76: 633-646.

Rose, K. D. 1981. The Clarkforkian land-mammal age and mammalian faunal composition across the Paleocene-Eocene boundary. University of Michigan Papers on Paleontology 26: 197 pp.

Walker, R. G. and D. J. Cant. 1984. Sandy Fluvial Systems. *In* R. G. Walker, ed. Facies models. Geological Association of Canada: 71-89.

TABLE 1
Comparison of diagnostic features
of Channel Lag Conglomerates and the SC-69 Sheetflood Conglomerate

	Channel Lag Conglomerate	Sheetflood Conglomerate
Clay Content in Matrix	Low	High
Framework Grain Types	Carbonate nodules, mudclasts, chert pebbles	Carbonate nodules, mudclasts
Sedimentary Structures	Crude cross-stratification	Crude cross-stratification w/ fine- and coarse-grained coupled foresets
Taphonomy	Isolated, abraded teeth w/ little to no carbonate encrustation	Isolated, abraded teeth w/ moderate carbonate encrustation; some teeth weathered into discoidal or spherical shapes; crushed dentary fragments; unabraded dentary fragments
Underlying Lithology and Contacts	Erosional contact often w/ low angle cross-stratified sandstone of sheet ss complex	Erosional contact w/ gray silty mudstone and ribbon sandstone of heterolithic deposit
Overlying Lithology and Contacts	Gradational contact w/ large-scale trough cross-stratified sandstone of sheet ss complex	Erosional contact w/ low angle cross-stratified sandstone of sheet ss complex

TABLE 2
Faunal list for the Sheetflood Conglomerate,
UMMP locality Sand Coulee 69 (SC-69)
of Wa-0/Wa-1 age (early Wasatchian, early Eocene).

Phylum MOLLUSCA

    Class GASTROPODA

        Gen. et sp. Indet

Phylum CHORDATA

    Class OSTEICHTHYES

        Order LEPISOSTEIFORMES

            Family Lepisosteidae

                Lepisosteus sp.

    Class MAMMALIA

        Order INSECTIVORA

            Family Nyctitheriidae

                Leptacodon rosei

        Order RODENTIA

            Gen. et sp. Indet

        Order TILLODONTIA

            Family Esthonychidae

                Esthonyx spatularius

        Order PANTODONTA

            Family Coryphodontidae

                Coryphodon sp.

Order CREODONTA

    Family Hyaenodontidae

        Arfia zele

        Prototomus phobos

        Prototomus martis

Order CARNIVORA

    Family Viverravidae

        Viverravus rosei

Order CONDYLARTHRA

    Family Arctocyonidae

        Chriacus gallinae

    Family Phenacodontidae

        Copecion davisi

        Ectocion osbornianus

        Ectocion parvus

Order ARTIODACTYLA

    Family Dichobunidae

        Diacodexis metsiacus

Order PERISSODACTYLA

    Family Equidae

        Hyracotherium grangeri

        Hyracotherium sandrae

TABLE 3
Faunal list for Channel Lag Conglomerate,
UMMP locality Sand Coulee 308 (SC-308)
of Wa-0/Wa-1 age (early Wasatchian, early Eocene)

Phylum CHORDATA
    Class OSTEICHTHYES
        Order LEPISOSTEIFORMES
            Family Lepisosteidae
                Lepisosteus sp.

    Class REPTILIA
        Order CROCODYLIA
            Family Alligatoridae
                Allognathosuchus sp.

    Class MAMMALIA
        Order MULTITUBERCULATA
            Family Eucosmodontidae
                Neoliotomus ultimus
        Order RODENTIA
            Gen. et sp. Indet

Order CREODONTA
    Family Hyaenodontidae
        Prototomus deimos
Order CONDYLARTHRA
    Family Arctocyonidae
        Chriacus gallinae
    Family Hyopsodontidae
        Haplomylus speirianus
        Hyopsodus loomisi
Order ARTIODACTYLA
    Family Dichobunidae
        Diacodexis metsiacus
Order PERISSODACTYLA
    Family Equidae
        Hyracotherium grangeri

Figure 1. Map of the "Upper Boundary Sandstone" (UBS), fossil sites associated with channel lag and sheetflood conglomerates, and UMMP Wa-0 fossil vertebrate localities at the southern tip of Polecat Bench in northwestern Wyoming. Paleoflow for the UBS was to NNE (11.47°). Note that the Wa-0 strata of SC-69 are nearly surrounded by fossiliferous conglomerates and that some conglomerate fossils were found several meters downhill upon Wa-0 strata (e.g. SC-308). A normal fault truncates the UBS in SC-308, which reappears on the boundary of SC-308/SC-67 and pinches out on the western edge of SC-67.

Figure 2. Correlated sections of pertinent Wa-0 localities at the southern end of Polecat Bench. The SC-67 section of Gingerich (2001) was used as a reference to which all other sections were compared. Dark gray shading within each section indicates the presence of a paleosol whereas the lighter gray represents overbank deposits associated with avulsion belts. The UBS scours downwards from the southeast (section SC-67) to the northwest and is thickest in SC-308/SC-405.

Figure 3. Representative examples of channel lag and sheetflood conglomerates. A) Weathered exposure of a channel lag conglomerate in the UBS at Polecat Bench exhibiting crude cross-strata and resting erosionally on a low-angle cross-stratified sandstone. B) A cleaned surface of the sheetflood conglomerate that exhibits weak bedding indicated by concentrations of large carbonate nodules. The conglomerate is 1 m thick at this exposure and rests upon a channel fill underlain by a basal sandstone lens. Note that the beds are nearly horizontal at the base of the conglomerate but exhibit

steeper angles higher up in the exposure. Vertical linear features are scratch marks produced from digging out the exposure. C) A weathered exposure of the sheetflood conglomerate showing a couplet consisting of a basal coarse grained bed overlain by a finer bed. The lower part of a second couplet overlies the first. D) A cleaned surface of the sheetflood conglomerate and underlying lithologies. A small sandstone lens rests erosionally upon Upper Double Red B, a distinctive Wa-0 red paleosol. Fine-grained deposits, with weak pedogenic alteration and a small sandstone body (lower outlined feature), overlie the sandstone lens. The sheetflood conglomerate is at the top of the exposure. The upper outlined feature is a clay lens within the conglomerate with conglomeratic material pushed into its top surface.

Figure 4. Representative mammalian fossils from the sheetflood conglomerate exhibiting various taphonomic features. A) A Hyracotherium grangeri (UM 113069) upper molar without roots or most of the marginal enamel, producing a discoidal grain. B) A well-rounded Copecion davisi M^3 (UM 113060) encrusted with calcium carbonate. Rounding occurred after encrustation by carbonate. C) A hyaenodontid dentary (UM 113094) with subparallel feeding traces and carbonate encrustation. D) A partial Hyracotherium grangeri dentary (UM 113067) that has been cracked, distorted, and cemented together with a sandy matrix similar to that of the conglomerate. No calcium carbonate encrustation appears on the dentary.

Figure 5. Schematic cross-section of the SC-69 conglomerate and associated lithologies. Heterolithic deposits (fine-grained overbank deposits and ribbon sandstones) lie

erosionally on Wa-0 paleosols, representing the development of a crevasse splay complex in SC-69 during an avulsion event. Fine-grained fill on the ribbon sandstone body indicates subsequent abandonment of the splay channel, producing a topographic low on the floodplain. Coarse grained sheetflood deposits, possibly resulting from severe flash floods, spread out over the splay and filled the abandoned splay channel. The sheetflood conglomerate was later truncated by the new trunk river established during the avulsion.

Figure 6. A.) Schematic setup of the contamination model. The stratigraphic range of a taxon is subdivided into 20 m bins, and the middle of each bin is assumed to be the fossiliferous source horizon. A fossil from interval $i+1$ is counted as a contaminant if it falls anywhere within interval i, meaning that Eq. 3 is evaluated from 10-30 m. B-D.) Predicted results for three scenarios in the contamination model. The magnitude of the observed species proportion relative to the median value is indicated by shading in each bin. If the presence of a taxon in interval i is not due to contamination than the true species proportion of the taxon will be positive ($p_{true} > 0$). B.) The observed proportions in intervals i and $i+1$ are both similar to the median proportion, and, therefore, the true proportion will be positive. C.) The observed proportion in interval i is significantly smaller than the proportion in interval $i+1$, producing a model result indicating the taxon is a contaminant in interval i. D.) The observed proportion in interval $i+1$ is significantly greater than the median proportion, artificially inflating the calculated contribution of contamination. Thus, the taxon of interest is erroneously seen as a contaminant in interval i.

Figure 7. The difference between observed species proportion and the proportion expected from contamination for <u>Ectocion osbornianus</u> and <u>Hyracotherium grangeri</u> plotted against stratigraphic level (black line). If the difference is ≤ 0, then the observed proportion can be explained by contamination alone. The gray line represents the difference between the species proportion of the overlying interval and the median species proportion as a means to detect biases in the test. The correlation will be negative if the contaminant contribution is biased by unusually large proportions in overlying intervals. Note that the presence of <u>E. osbornianus</u> and <u>H. grangeri</u> in Wa-0 interval can be explained by contamination alone.
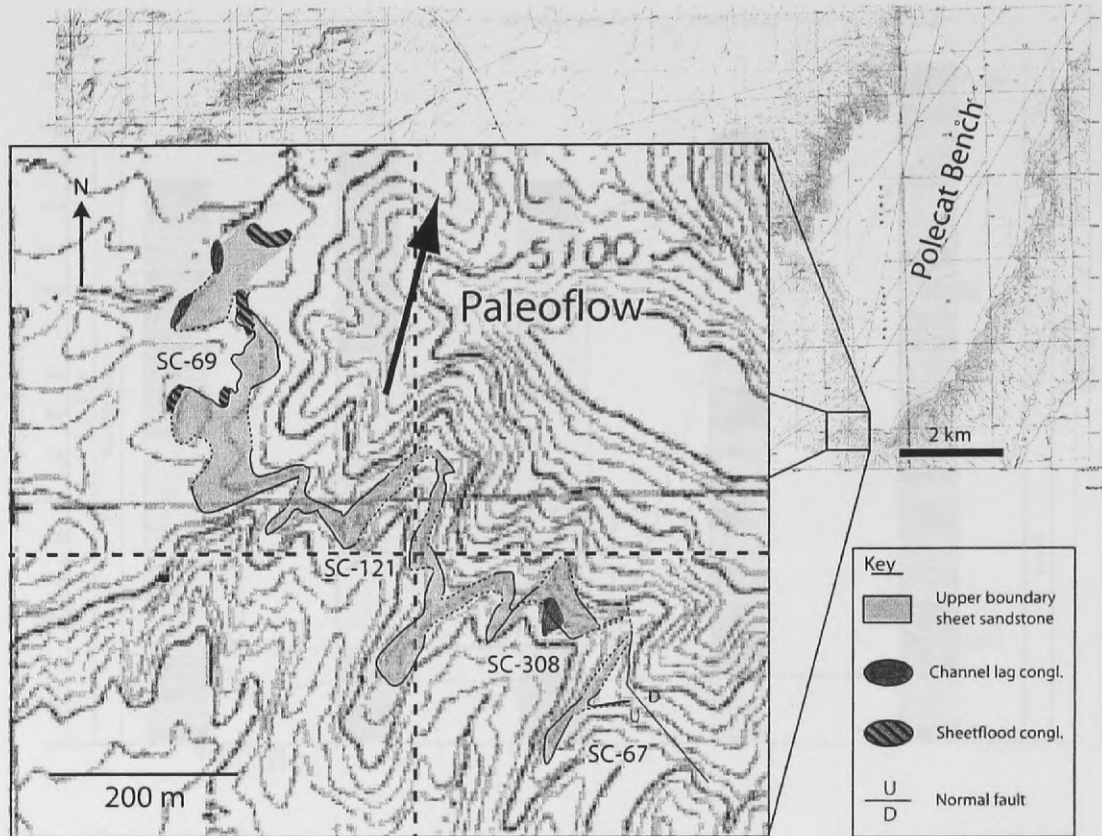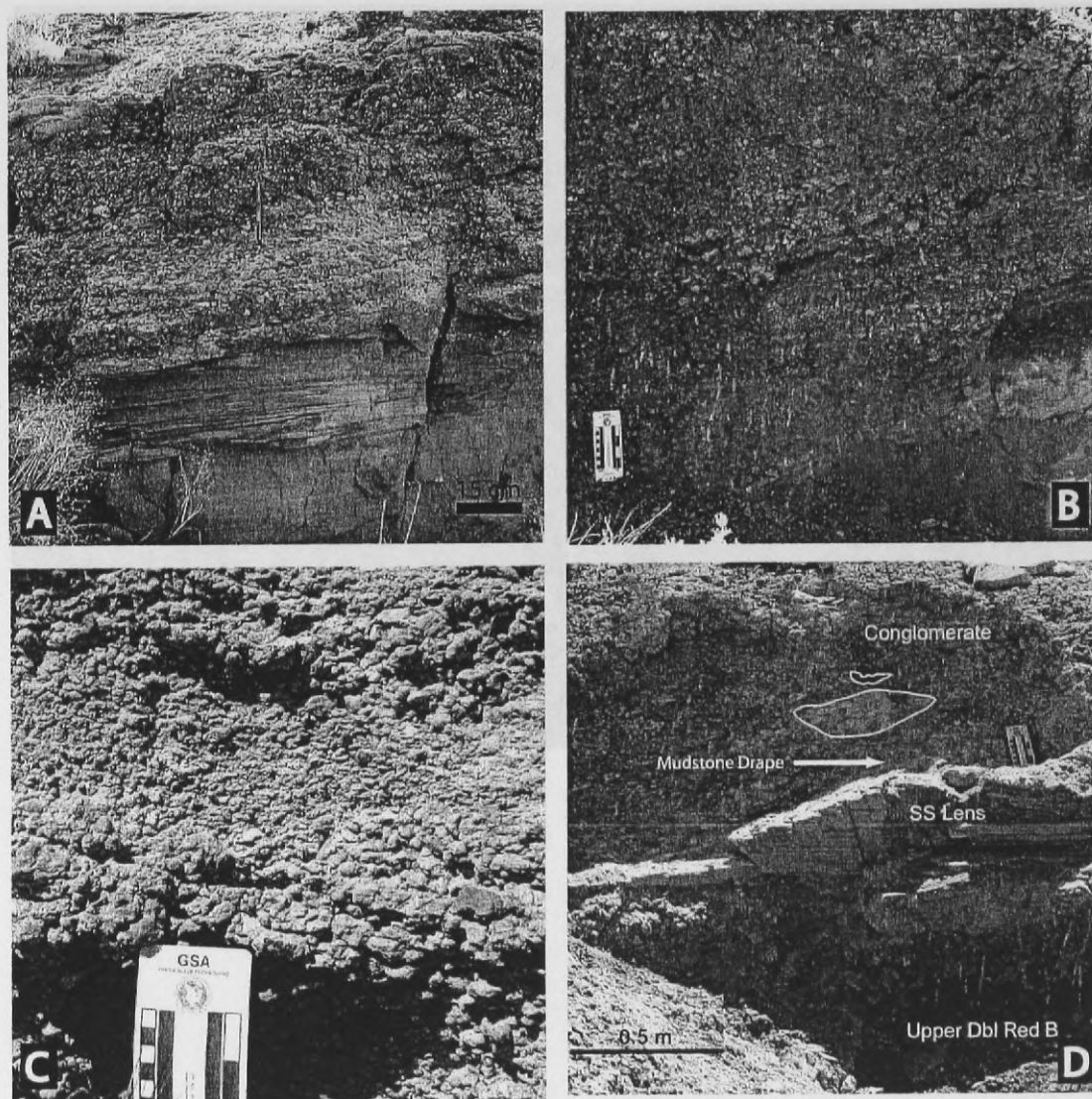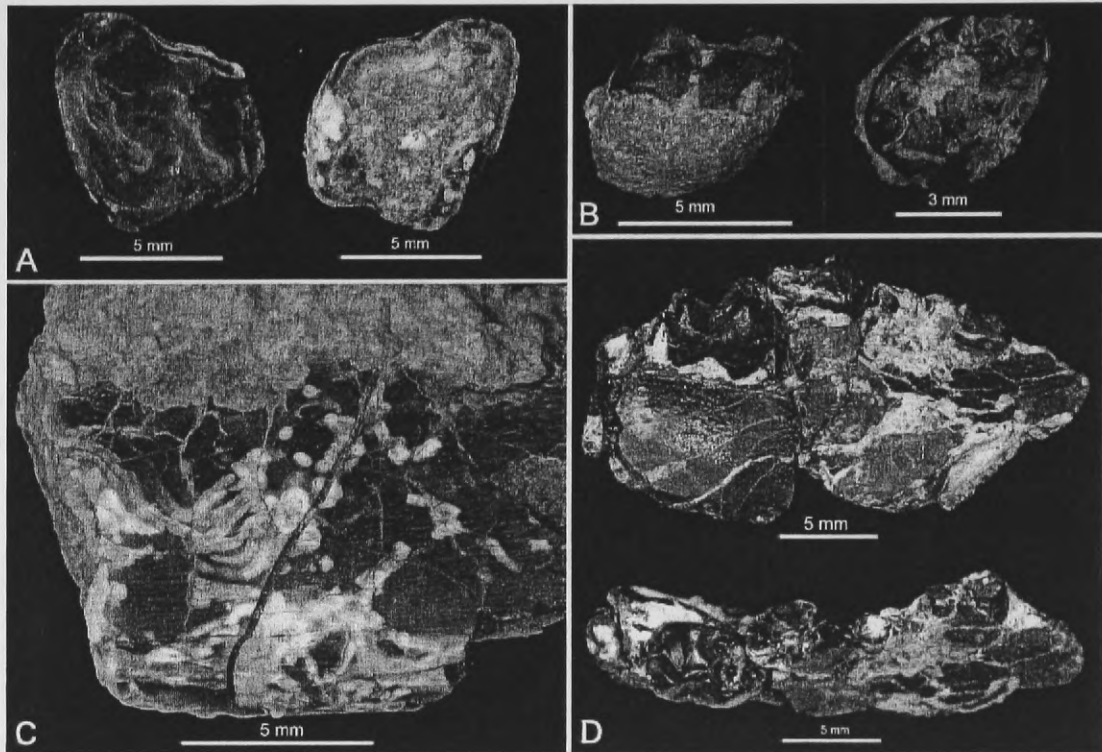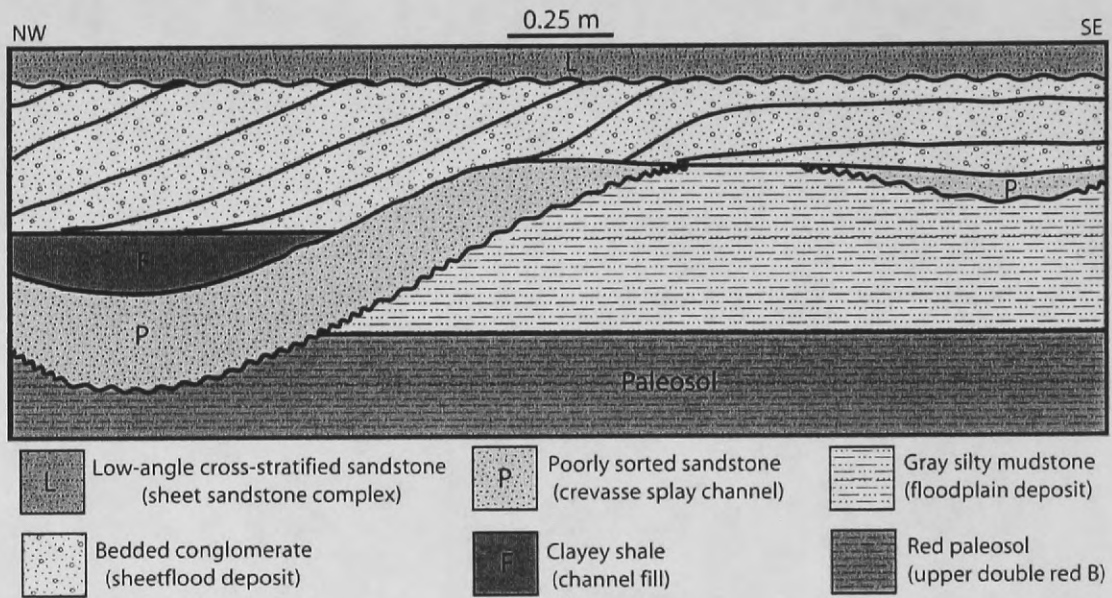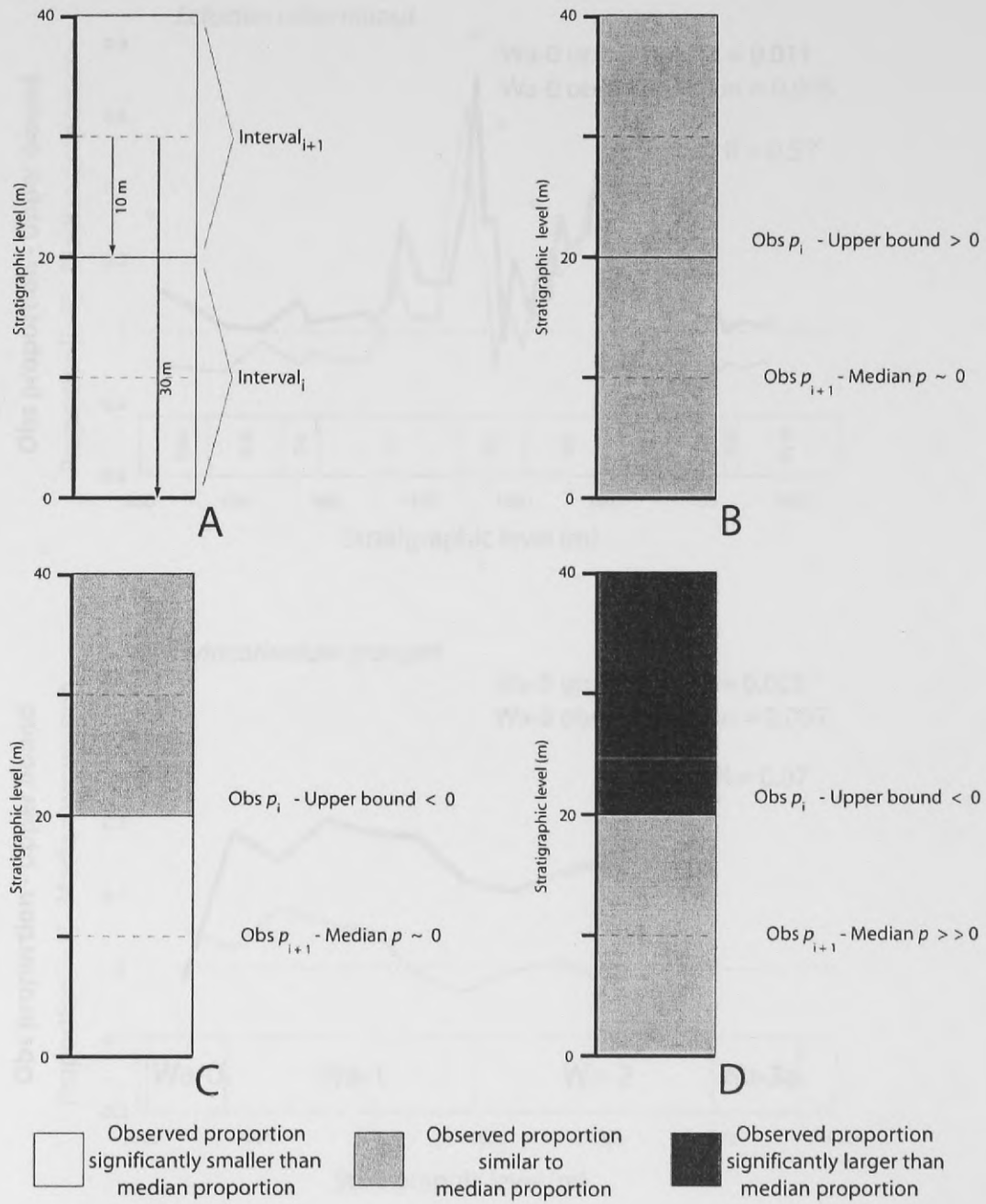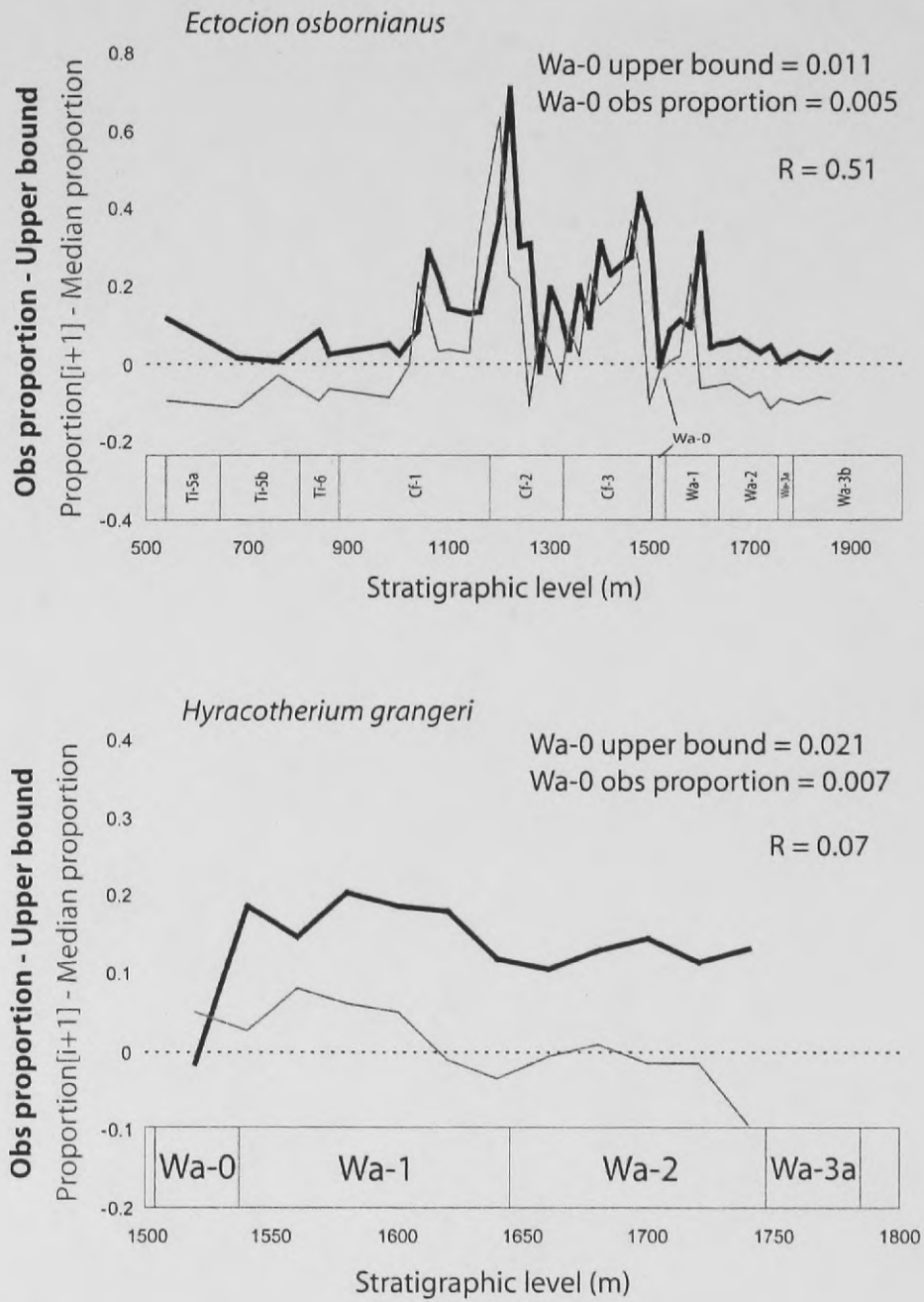
Figure 1.
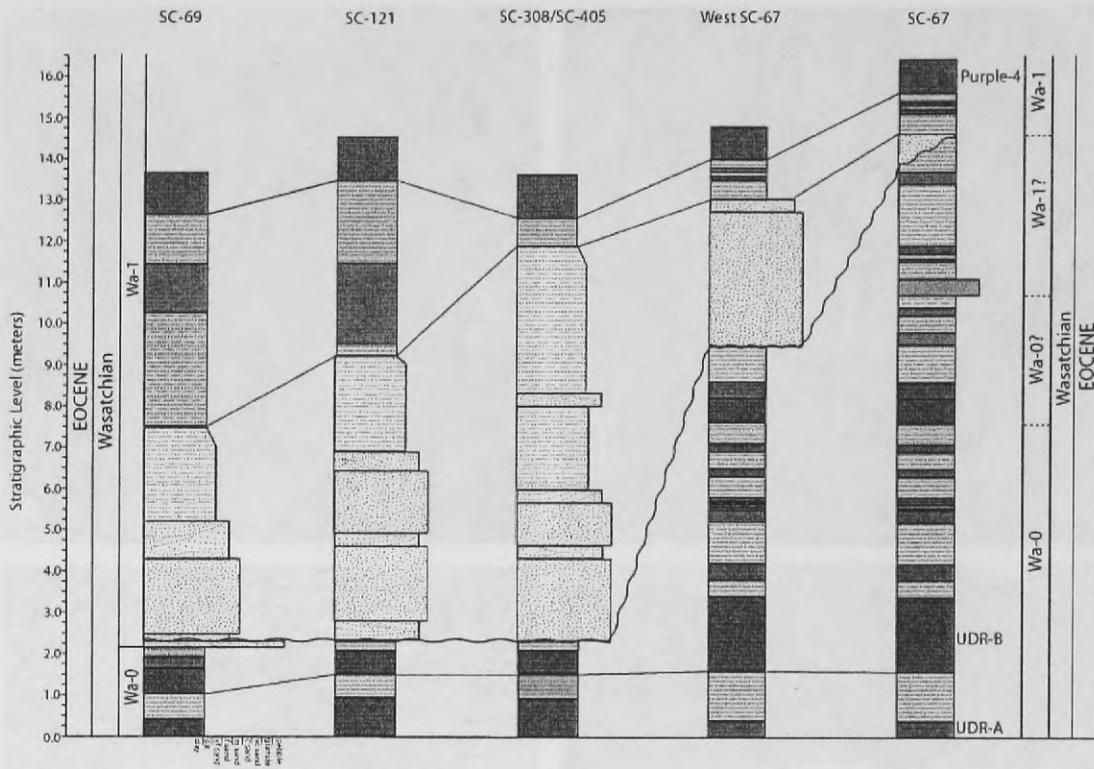
Figure 2.

Figure 3.

Figure 4.

Figure 5.

Figure 6.

Ectocion osbornianus

Wa-0 upper bound = 0.011
Wa-0 obs proportion = 0.005

R = 0.51

Hyracotherium grangeri

Wa-0 upper bound = 0.021
Wa-0 obs proportion = 0.007

R = 0.07

Figure 7.